Isoprenoids determine Th1/Th2 fate in pathogenic T cells, providing a mechanism of modulation of autoimmunity by atorvastatin

Shannon E. Dunn,[1] Sawsan Youssef,[1] Matthew J. Goldstein,[1] Thomas Prod'homme,[2] Martin S. Weber,[2] Scott S. Zamvil,[2] and Lawrence Steinman[1]

[1]Department of Neurology and Neurological Sciences, Stanford University, Stanford, CA 94305
[2]Department of Neurology, University of California San Francisco, CA 94143

3-hydroxy-3-methylglutaryl–coenzyme A (HMG-CoA) reductase is a critical enzyme in the mevalonate pathway that regulates the biosynthesis of cholesterol as well as isoprenoids that mediate the membrane association of certain GTPases. Blockade of this enzyme by atorvastatin (AT) inhibits the destructive proinflammatory T helper cell (Th)1 response during experimental autoimmune encephalomyelitis and may be beneficial in the treatment of multiple sclerosis and other Th1-mediated autoimmune diseases. Here we present evidence linking specific isoprenoid intermediates of the mevalonate pathway to signaling pathways that regulate T cell autoimmunity. We demonstrate that the isoprenoid geranylgeranyl–pyrophosphate (GGPP) mediates proliferation, whereas both GGPP and its precursor, farnesyl–PP, regulate the Th1 differentiation of myelin–reactive T cells. Depletion of these isoprenoid intermediates in vivo via oral AT administration hindered these T cell responses by decreasing geranylgeranylated RhoA and farnesylated Ras at the plasma membrane. This was associated with reduced extracellular signal–regulated kinase (ERK) and p38 phosphorylation and DNA binding of their cotarget c-fos in response to T cell receptor activation. Inhibition of ERK and p38 mimicked the effects of AT and induced a Th2 cytokine shift. Thus, by connecting isoprenoid availability to regulation of Th1/Th2 fate, we have elucidated a mechanism by which AT may suppress Th1-mediated central nervous system autoimmune disease.

Recently, it was reported that oral administration of simvastatin (Zocor) reduced the expected number of new gadolinium-enhancing lesions in relapsing-remitting multiple sclerosis (MS) patients by 44% in a small 6-mo open-label trial (1). The related drug atorvastatin (AT) (Lipitor) has also shown promising results in lowering disease scores and vascular risk factors in patients with rheumatoid arthritis (2) and is currently being tested in MS in a multi-center, placebo-controlled trial (http://www.immunetolerance.org/trials) (3). Studies in experimental autoimmune encephalomyelitis (EAE) (4–8) and other animal models of Th1-mediated disease (9, 10) have revealed that statin drugs interfere with the autoimmune de-

struction of target tissues by inhibiting multiple arms of the immune response.

In EAE, statins prevent the production of inflammatory mediators TNF-α, IFN-γ, and iNOS by astrocytes and microglia in the central nervous system (CNS) (4) and blunt inducible expression of MHCII and costimulatory molecules by these cells (5). These drugs also affect T cells, the initiators of the autoimmune process, by preventing their expansion, Th1 differentiation, and migration across the blood–brain barrier (5–8). When myelin-reactive CD4+ T cells are primed with antigen in the presence of statins, they instead secrete lower amounts of TNF-α and the Th1 cytokine IFN-γ and higher amounts of protective Th2 cytokines such as IL-4 (5, 6, 8). Adoptive transfer studies have demonstrated that AT-generated, myelin-reactive Th2 cells have a limited capacity to migrate into the CNS (unpublished data) and provide sustained

S.E. Dunn and S. Youssef contributed equally to this work.
S.S. Zamvil and L. Steinman contributed equally to this work.
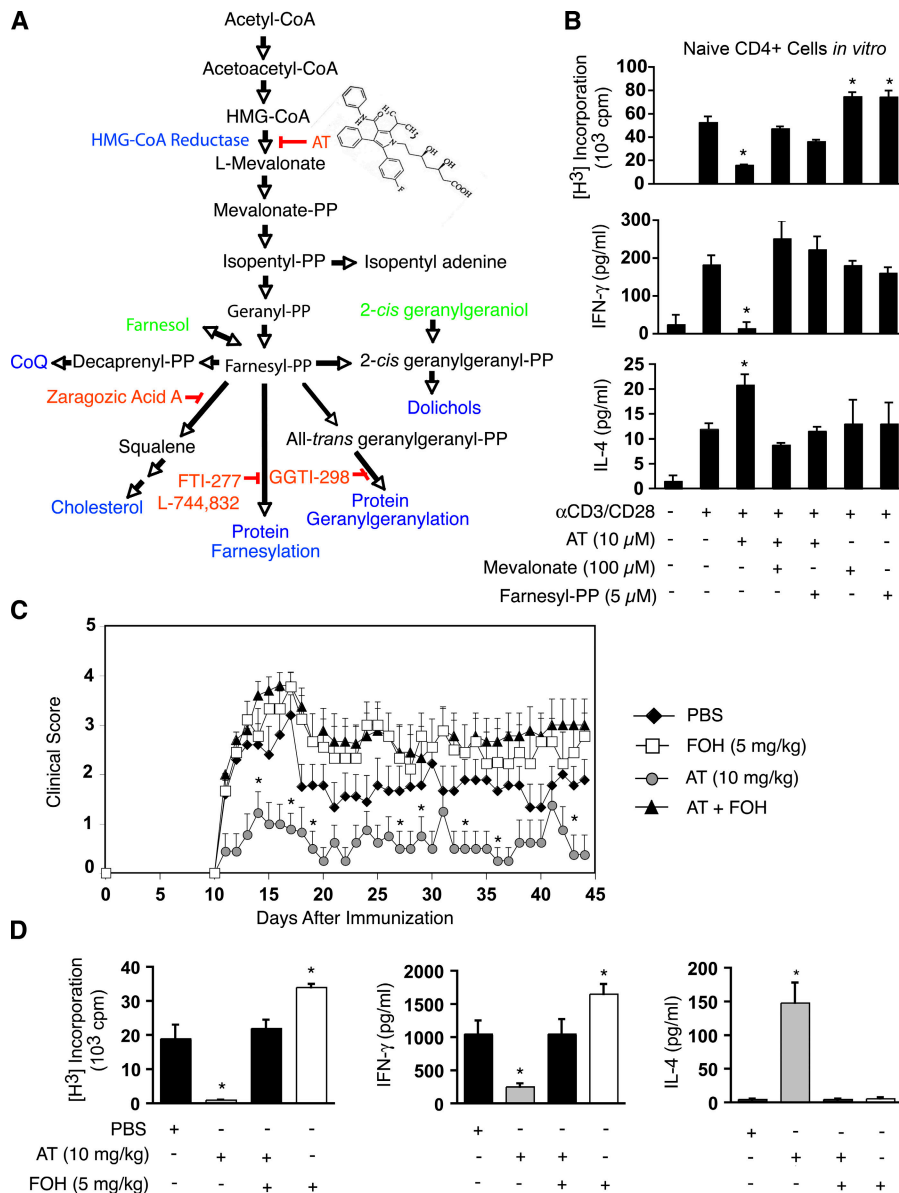The online version of this article contains supplemental material.

Figure 1. The mevalonate pathway intermediate farnesyl–PP and its alcohol precursor farnesol reverse the Th2 bias promoted by atorvastatin. (A) The mevalonate pathway. Metabolites and enzymes in the pathway are shown in black, drug inhibitors are shown in red, alcohol precursors to metabolites are shown in green, and HMG-CoA reductase and pathway end-products are shown in blue. CoQ, coenzyme Q10/ubiquinone. (B) Purified naive B10.PI CD4$^+$ cells stimulated with 5 μg/ml αCD3/αCD28 were cultured in the presence or absence of 10 μM atorvastatin (AT), 100 μM mevalonate, or 5 μM farnesyl–PP. Proliferation (top) was measured by [^{3}H]-thymidine incorporation, and IFN-γ (middle) and IL-4 (bottom) accumulation in culture supernatants were measured by ELISA. These metabolite doses were optimal in reversal of AT effects.

Values are mean ± SE of three cultures. Results are representative of three independent experiments. *, denotes a significant (P < 0.05) difference from αCD3/αCD28 stimulation group. (C and D) Female SJL mice (n = 10/group) were immunized with PLP p139-151 in CFA and daily were fed PBS or AT (10 mg/kg) and/or were injected with farnesol (FOH) (5 mg/kg, i.p.). At day 10 after immunization, two spleens were taken from representative mice in each group and pooled, and isolated splenocytes were cultured ex vivo with PLP p139-151 peptide. C shows the mean ± SE clinical scores of these mice, whereas D shows the proliferation of [^{3}H] incorporation (left), IFN-γ (middle), and IL-4 (right) production by these cells. *, denotes a significant difference from (P < 0.05) PBS control.

protection from further attacks of paralysis (5). Interestingly, a similar bias toward a higher ratio of Th2/Th1 CD4$^+$ cells in peripheral blood has been observed in human cardiac patients receiving low–dose (20 mg/d) AT therapy (11).

Despite these advances, the molecular mechanism by which statins modulate T cell immunity is unknown. This is important given the broad clinical administration of these agents (∼25 million people world–wide) (12). Identified

protein targets of these drugs include 3-hydroxy-3-methylglutaryl–coenzyme A (HMG-CoA) reductase, a rate-limiting enzyme in the mevalonate pathway that generates cholesterol and isoprenoid derivatives (Fig.1 A) (13, 14) and the integrin, leukocyte function antigen-1 (15). In the present study, we provide novel evidence that the Th2 bias promoted by AT is the result of a reduction of the mevalonate pathway-derived isoprenoids, farnesyl-pyrophosphate (PP) and all-trans geranylgeranyl-PP in T cells. These lipid derivatives are known to covalently attach to and mediate the membrane association of certain signaling proteins and metabolites in cells (13, 14). We show that in vivo depletion of these lipids in EAE mice via oral AT administration prevented the membrane association of farnesylated Ras and geranylgeranylated RhoA, but not other GTPases in lymph node cells. This was associated with compromised TCR–induced activation of Ras and RhoA effectors such as extracellular signal–regulated kinase (ERK), p38, and their cotarget c-fos. Because c-fos (as part of AP-1) transactivates the IFN-γ promoter and represses the IL-4 promoter (16), our results explain how AT can bias naive CD4$^+$ T cells to produce relatively higher amounts of IL-4 in the early period of antigen signaling and thus trigger the Th2 program of differentiation. By connecting specific isoprenoids in the mevalonate pathway to T cell receptor signaling pathways that regulate cytokine production, we have elucidated a mechanism of how statins may inhibit Th1-mediated autoimmunity.

RESULTS

AT prevents Th1 differentiation of CD4$^+$ cells by targeting HMG–CoA reductase

Previous reports have shown that the effect of AT in T cells is reversed by mevalonate (5, 6), suggesting that the actions of this drug may be mediated through inhibition of HMG-CoA reductase (Fig. 1 A). However, because statins are structurally similar to mevalonate and have other ligands on immune cells (i.e., leukocyte function antigen-1) (15), it is also possible that such a reversal is a result of competition between mevalonate and AT for binding on protein targets other than HMG-CoA reductase. We thus tested whether the effects of AT on T cells could also be reversed by farnesyl-PP, the last common intermediate in the mevalonate pathway that has a different structure than mevalonate. In response to αCD3/αCD28 costimulation, purified naive (CD62L$^+$/CD44^{low}) CD4$^+$ T cells proliferated and differentiated to secrete high amounts of the Th1 cytokine IFN-γ (Fig. 1 B). As shown previously (5, 6, 8), AT blunted these T cell responses and enhanced their production of IL-4 (Fig. 1 B). Farnesyl-PP, like mevalonate, fully reversed the effects of AT and, when administered alone, enhanced the TCR-induced proliferation of CD4$^+$ cells (Fig. 1 B).

Paralleling these in vitro findings, administration of farnesol, a lipophilic, alcohol precursor to farnesyl-PP (17), reversed the clinical and immune modulatory effects of AT in vivo during EAE (Fig. 1, C and D, and Table S1, available
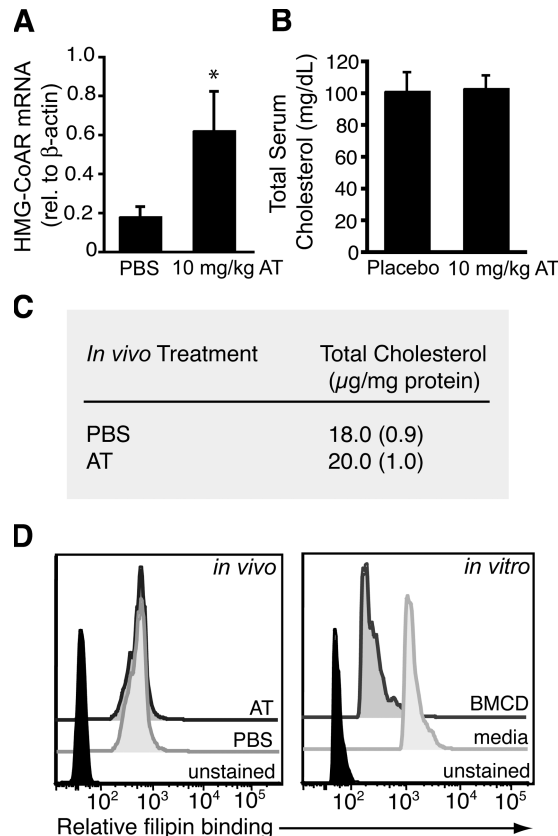

Figure 2. Oral atorvastatin treatment does not affect circulating or T cell cholesterol. (A) B10.PL mice ($n = 4$/group) were treated with either PBS or 10 mg/kg atorvastatin (AT) for 30 d after which time the liver was removed and HMG-CoA reductase (HMG-CoAR) transcript levels were assessed using real-time RT-PCR. *, denotes a significant difference (P < 0.05) from PBS liver. (B) Serum levels of total cholesterol (mg/dL) in mice treated orally with PBS or AT (10 mg/kg). Serum was taken from mice at 5 d after treatment in the morning after an overnight fast. Values are mean ± SE of five mice. (C) T cells were isolated from the spleens of mice treated as in B and total cholesterol (μg/mg protein) was measured in lipid extracts of these cells using the Amplex Red Cholesterol Assay. (D) Flow cytometric analysis of filipin staining in purified T cells taken from mice treated as in B (left) or in T cells that were incubated in vitro in serum-free media for 2 h with the cholesterol-depleting agent β-methyl-cyclodextrin (BMCD) (right). The latter experiment served as a positive control to demonstrate the sensitivity of this assay to detect cholesterol changes.

at http://www.jem.org/cgi/content/full/jem.20051129/DC1). Interestingly, myelin (PLP p139-151)-reactive cells taken from mice treated with farnesol alone also proliferated more vigorously and secreted higher amounts of IFN-γ ex vivo in response to stimulation with specific peptide (Fig. 1 D). Collectively, these findings confirm that AT modulates the Th differentiation of CD4$^+$ cells by inhibiting the production of an intermediate in the mevalonate pathway. They also suggest that accumulation of farnesyl-PP in response to farnesol treatment may enhance the expansion of Th1 effector cells.
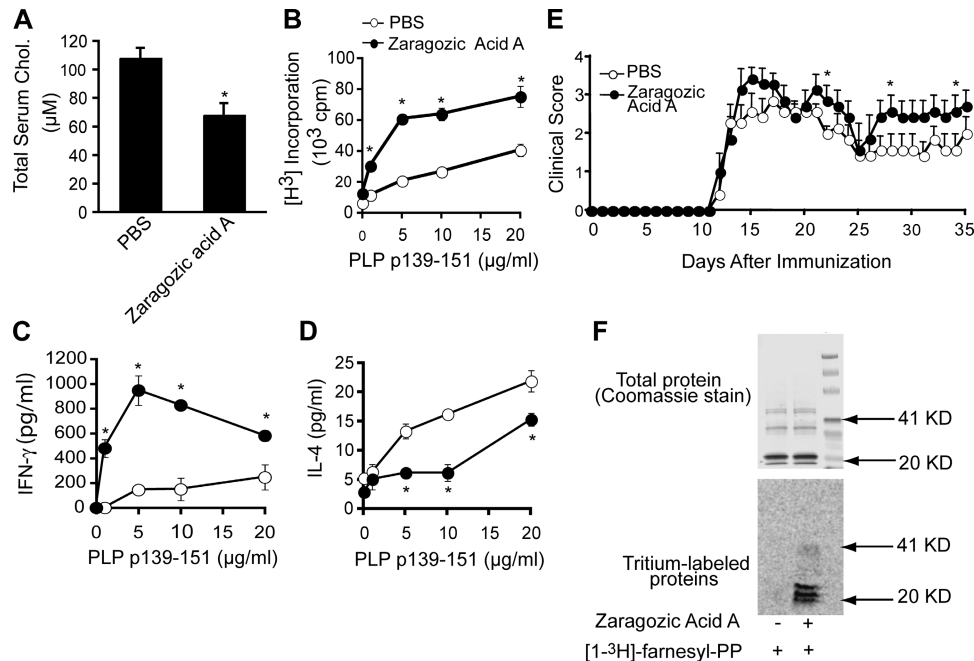
Figure 3. Specific inhibition of the sterol branch of the mevalonate pathway enhances T cell proliferation and Th1 differentiation. SJL mice ($n = 10$/group) were immunized with PLP p139-151 in CFA and were injected once daily with either PBS or Zaragozic Acid A (10 mg/kg, i.p.). At day 10 after immunization, axillary, brachial, and inguinal lymph nodes were taken from representative mice in each group and pooled, and isolated cells were cultured ex vivo with PLP p139-151 peptide. (A) Total cholesterol (μM) in serum taken at the peak of disease activity. Values are mean $\pm$ SE of five mice. (B–D) Proliferation of PLP p139-151 reactive cells (B) was measured by [³H]-thymidine incorporation, and IFN-γ (C) and IL-4 (D) accumulation in culture media was measured by ELISA. Values are mean $\pm$ SE of three cultures. (E) Mean $\pm$ SE clinical scores of mice in the various groups over the time-course of disease are shown. *, denotes a difference ($P < 0.05$) from PBS control. (F) De novo incorporation of [1-³H]-farnesyl-PP into cellular proteins in the absence or presence of Zaragozic Acid A (200 μM) in T cell cultures. The protein marker is in lane 3 (top). Gels were stained with Coomassie blue to ensure that equivalent amounts of each protein sample were loaded.

Effects of AT on T cell growth and differentiation are independent of cholesterol reduction

Cholesterol is a major product of farnesyl-PP (Fig. 1 A). Although it has been reported that depletion of this lipid in T cells can attenuate TCR signaling by disruption of cholesterol-rich lipid rafts (18), a recent in vitro study of malignant T cells showed lipid raft disruption by statins only in the complete absence of exogenous cholesterol in the media (19). We found that in the context of the whole organism, AT treatment (10 mg/kg) reduced the production of this metabolite by the liver as indicated by an elevation in the mRNA expression of HMG-CoA reductase (this gene is negatively regulated by sterols in this tissue; reference 13) (Fig. 2 A). However, the total amount of cholesterol in the serum or in T cells was unchanged by this treatment (Fig. 2, B and C). The level of membrane-associated cholesterol was also not altered in T cells in response to oral administration of this drug as assessed via flow cytometric analysis of filipin staining (Fig. 2 D, left). The lack of detectable change in membrane cholesterol with AT was not a result of limits in the sensitivity of this assay, because decreased filipin fluorescence was observed in T cells incubated in serum-free media with the cholesterol-depleting agent β-methyl cyclodextrin (Fig. 2 D, right).

To more specifically address the role of the sterol branch of the mevalonate pathway in immunomodulation, we examined the effects of the squalene synthetase inhibitor Zaragozic Acid A (10 mg/kg) on encephalitogenic T cell responses during EAE. At this dose, Zaragozic Acid A inhibits liver sterol synthesis (20), reduces circulating cholesterol (Fig. 3 A) and at the same time causes an accumulation of farnesol in mice (20). Daily subcutaneous injection of mice with Zaragozic Acid had opposite effects to AT and caused PLP p139-151–reactive cells to proliferate more vigorously (Fig. 3 B) and secrete higher amounts of IFN-γ (Fig. 3 C) and lower amounts of IL-4 (Fig. 3 D) compared with PBS-injected counterparts. Zaragozic Acid A treatment also exacerbated EAE at several time-points in disease (Fig. 3 E and Table S2, available at http://www.jem.org/cgi/content/full/jem.20051129/DC1).

To examine whether the enhanced proliferation of Th1 cells triggered by Zaragozic Acid A was a result of enhanced flux of farnesyl-PP into isoprenoid branches of the pathway, we investigated the effect of this drug on the de novo incorporation [1-³H] farnesyl-PP into T cell proteins in vitro. We found that in comparison to media control, Zaragozic Acid A–treated T cells displayed an increased abundance of tritium-labeled proteins in the 21–29 kD range, which is compatible
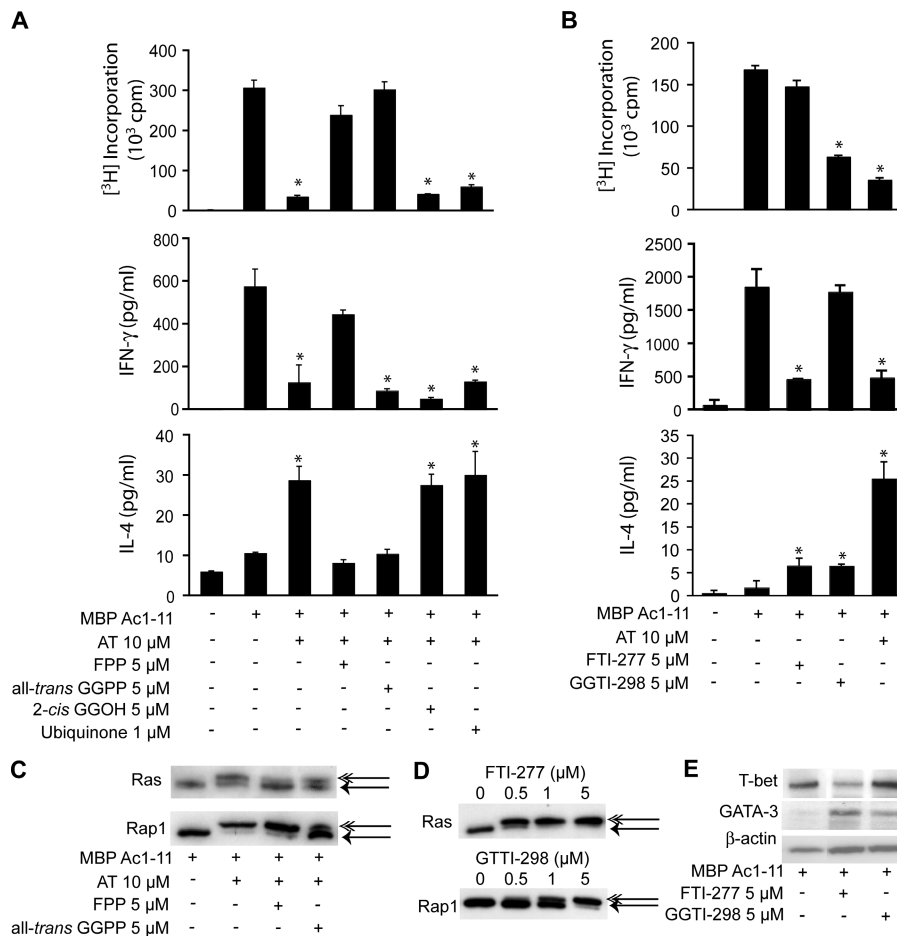
Figure 4. Prenylated proteins have a regulatory function in T cell growth and differentiation. (A and B) Splenocytes taken from MBP Ac1-11 TCR Tg mice were stimulated with 5 μg/ml Ac1-11 peptide in the presence or absence of 10 μM atorvastatin (AT), 5 μM farnesyl-PP (FPP), 5 μM all-trans geranylgeranyl-PP (all-trans GGPP), 1 μM 2-cis geranyl-geraniol (2-cis GGOH), or 1 μM ubiquinone (all in A) or DMSO vehicle, 5 μM of the farnesyltransferase inhibitor FTI-277 or 5 μM of the geranyl-geranyltransferase-I inhibitor GGTI-298 (all in B). Proliferation (top) was measured by [³H]-thymidine incorporation, and IFN-γ (middle), and IL-4 (bottom) accumulation in culture supernatants was measured via ELISA. These results are representative of data from at least three independent experiments. *, denotes a difference (P < 0.05) from peptide stimulation alone. Note that the additive effects of FTI and GGTI were not examined in these experiments because this drug combination compromised T cell viability (not depicted). Values are mean ± SE of triplicate cultures. (C) 5 μM farnesyl-PP is effective at restoring the prenylation of Ras, a representative farnesylated protein and 5 μM all-trans GGPP is effective at restoring the prenylation of Rap, a representative geranylgeranylated protein. Because the carboxy-termini of these proteins are cleaved upon prenylation, posttranslationally modified forms (single arrows) of these proteins can be distinguished from their unprenylated forms (double arrows) via altered mobility on Western blots of SDS-PAGE gels (reference 27). (D) 1 and 5 μM of FTI-277 and 5 μM GGTI-298, respectively, inhibit Ras farnesylation and Rap1 geranylgeranylation. (E) Protein samples from cells treated with FTI, GGTI, or vehicle control (as in B) were subjected to Western blot analysis of T-bet and GATA-3 expression.

with the size of small G proteins (Fig. 3 F). Collectively, these results suggest that the major effects of AT on Th1 differentiation and clinical disease are cholesterol independent and instead the result of reductions in isoprenoid biosynthesis.

AT inhibits T cell growth and Th1 differentiation by preventing protein isoprenylation

Farnesyl-PP serves as a metabolic precursor to a variety of isoprenoid derivatives such as decaprenyl-PP (isoprenoid moiety of ubiquinone), 2-cis-geranylgeranyl-PP (important for N-glycoprotein synthesis), and all-trans geranylgeranyl-PP (13, 14) (Fig. 1 A). The latter isoprenoid along with farnesyl-PP are, respectively, attached to the COOH terminus of certain signaling proteins via the action of geranylger-anyl transferases and farnesyltransferase (21). These isoprenoid modifications mediate the membrane association of many GTPases (21). We thus tested whether specific isoprenoid derivatives could reverse the effects of AT on T cells cultured with specific peptide. Splenocytes from MBP Ac1-11 TCR transgenic (Tg) mice were used as a source of T cells for these assays.

Of all the metabolites tested, only all-trans geranylgeranyl-PP, the isoprenoid moiety of geranylgeranylated proteins, and its precursor, farnesyl-PP, restored the antigen-driven

proliferation of AT-treated T cells and reversed the Th2 bias promoted by this drug (Fig.4 A). The doses of farnesyl-PP and geranylgeranyl-PP used in these assays were effective at restoring the prenylation of protein targets (Fig. 4 C). We also tested the effects of these isoprenoids in AT-treated T cells stimulated with α-CD3 and α-CD28 (Fig. S1, available at http://www.jem.org/cgi/content/full/jem.20051129/DC1) and found that both farnesyl-PP and geranylgeranyl-PP contributed to the reversal of AT effects on T cell proliferation and Th1 differentiation. Collectively, these data strongly suggest that AT modulates Th differentiation by inhibiting isoprenoid production in T cells.

To confirm the involvement of isoprenylated proteins in T cell growth and Th1 differentiation, we investigated the effects of inhibitors of farnesyltransferase (FTI-277) and geranylgeranyltransferase-I (GGTI-298) on antigen-driven T cell responses (Fig. 4, B and D). Treatment of MBP Ac1-11 TCR Tg T cells with an effective dose (Fig. 4 D) of the geranylgeranyltransferase inhibitor (GGTI) significantly inhibited T cell proliferation (Fig. 4 B). However, the growth of these cells was not altered by treatment with the farnesyltransferase inhibitor (FTI) (Fig. 4 B). Consistent with the prominent involvement of protein farnesylation in regulating Th1 differentiation, FTI-277 inhibited the production of IFN-γ and induced a subtle increase in IL-4 by T cells (Fig. 4 B). In parallel, this drug decreased T-bet protein and caused a subtle increase in GATA-3 expression (Fig. 4 E). GGTI-298, though not influencing IFN-γ secretion or T-bet expression, induced low-level IL-4 production and a subtle increase in GATA-3 expression (Fig. 4, B and E). Similar effects of FTI-277 and GGTI-298-treatment on T proliferation and cytokine production were observed in cultures of purified T cells stimulated with anti-CD3 and anti-CD28 (Fig. S1). Note that in both of these T cell assays, the amount of IL-4 triggered by each of these prenyltransferase inhibitors did not approach the level induced by AT (Fig. 4 B and Fig. S1), suggesting that geranylgeranylated proteins cooperate with farnesylated proteins to fully repress the production of this Th2 cytokine in T cells in response to antigen signals. Collectively, these results suggest that AT prevents T cell proliferation and Th1 differentiation by inhibiting the biosynthesis of farnesyl-PP and all-trans geranylgeranyl-PP, leading to reduced prenylation of protein targets.

Oral AT administration promotes a Th2 bias by decreasing the membrane association of Ras and RhoA

Farnesylated Ras and geranylgeranylated Rac1, RhoA, and Rap are the only prenylated proteins known to be situated in antigen-activated signaling pathways that modulate T helper differentiation (22). Though numerous in vitro studies of malignant cells have demonstrated an inhibitory effect of high-dose (10–50 μM) statin treatment on the prenylation and membrane-association of Ras and Rho GTPases (e.g., 19, 23, 24), a similar in vivo effect of statins on these proteins has not been reported. We thus investigated whether oral AT administration altered the subcellular localization of Ras,
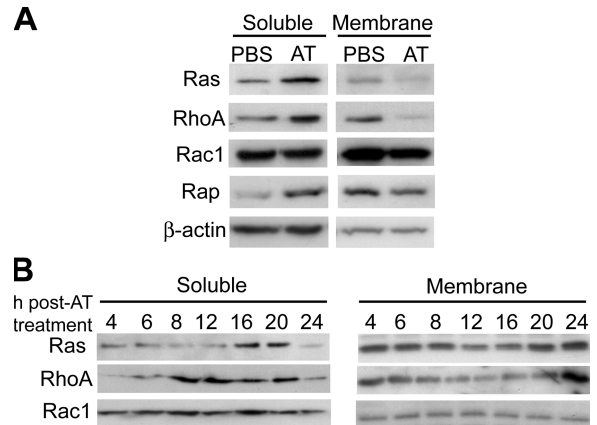

Figure 5. Oral atorvastatin treatment decreases the membrane association of Ras and RhoA GTPases. (A) Lymph node cells were taken from five (SJL×PLJ)$_{F1}$ mice that had been immunized 10 d previously with MBP Ac1-11 in CFA. These mice had been fed daily with either PBS or AT (10 mg/kg). At 16 h after the last dosing, lymph nodes were taken from mice and pooled, and the soluble and membrane fractions of these cells were separated by ultracentrifugation (100,000 g). Proteins were subjected to SDS-PAGE electrophoresis and Western blot analysis of Ras, RhoA, Rap, Rac1, and β-actin was performed. (B) B10.PI mice (n = 2/group) were fed with AT (10 mg/kg) once daily for 3 d. After the third treatment, spleens were taken from mice at different time points. Splenocytes were isolated, the soluble and membrane fractions were obtained, and Western blot analysis of Ras, RhoA, and Rac1 expression was performed as in A.

RhoA, Rac1, or Rap in T cells in vivo during EAE. We used draining lymph nodes from EAE mice as a source of enriched T cells. We found that AT treatment induced an accumulation of Ras, Rap, and RhoA, but not Rac1 in the cytosol of draining lymph node cells (Fig. 5 A). This was accompanied by a prominent decrease in Ras and RhoA at the membrane (Fig. 5 A). This effect of AT on Ras and Rho was reversed by coadministering farnesol to mice (Fig. S2 A, available at http://www.jem.org/cgi/content/full/jem.20051129/DC1). Time-course experiments demonstrated that the alteration in Ras and RhoA localization in immune cells by AT was transient (Fig. 5 B) and occurred as early as 6 h (not depicted) and as late as 20 h (Fig. 5 B) after oral treatment. Because membrane localization is requisite to the functioning of these proteins, our findings strongly implicate Ras and RhoA as the major targets of AT in immune modulation.

It has been suggested that early cytokine production by naive CD4$^+$ cells in response to antigen stimulation may be influenced by the extent of activation of the Ras–ERK signaling pathway downstream of the TCR (16, 25). In response to strong TCR signals, Ras and ERK are activated in a sustained fashion leading to increased c-fos activity (16, 25). c-fos (together with jun proteins such as AP-1) transactivates the IFN-γ promoter and may repress the IL-4 promoter (16) (Fig. 6 A). Decreased RhoA activation may also tip cytokine balance toward Th2 via inhibition of p38, a kinase that positively regulates IFN-γ production (26) (Fig. 6 A). We thus
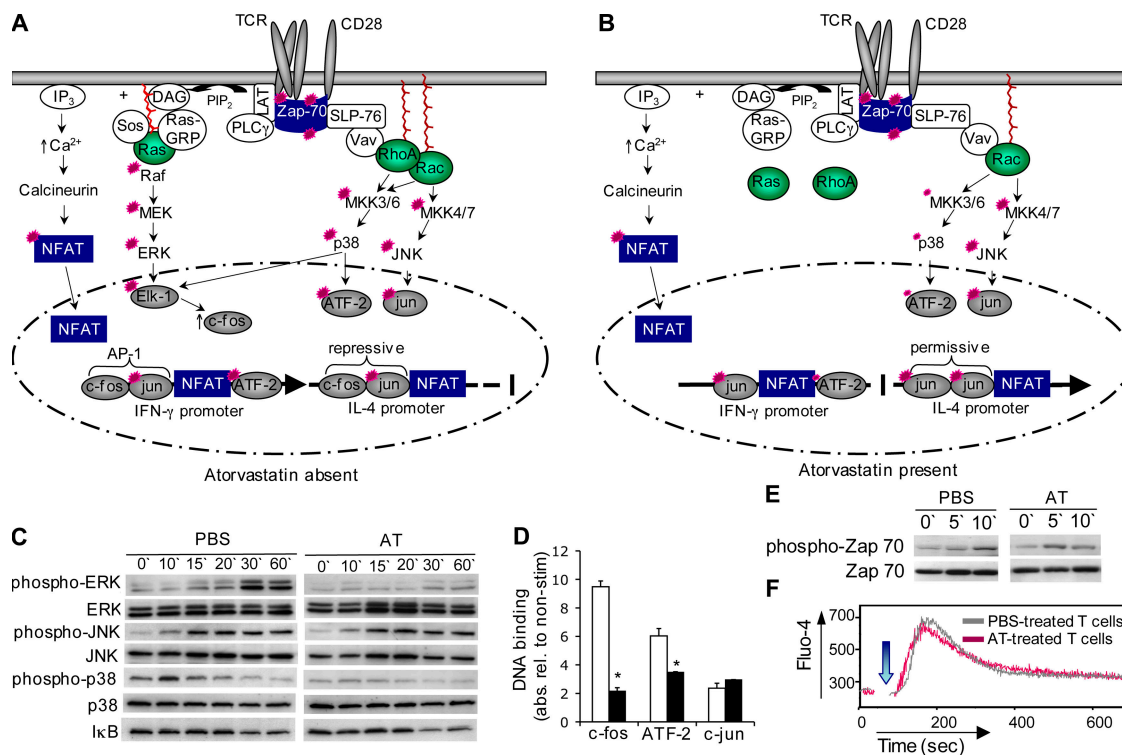
Figure 6. Oral atorvastatin treatment inhibits ERK and p38 signaling pathways in T cells. (A and B) Cartoon summarizing the location of prenylated proteins (in green) in signaling pathways downstream of TCR stimulation and the transcription factors that act at IFN-γ and IL-4 promoters in PBS- (A) and AT-dosed (B) mice. Not all pathway intermediates are shown. (C–E) Lymph node cells (C and D) or purified CD4+ cells (E) taken from mice treated as in Fig. 5 were cultured (2 × 10⁶/ml) with 5 μg/ml αCD3 and 5 μg/ml αCD28 antibodies for various durations. (C) Western blot analysis of phospho-ERK, ERK, phospho-JNK, JNK, phospho-p38, p38 MAPK, and IκB using whole cell lysates prepared from these cells. (D) shows results of an ELISA-based DNA binding assay of c-fos, ATF-2, and c-jun using nuclear extracts prepared from parallel cultures that were stimulated with 5 μg/ml αCD3/αCD28 antibodies for 10 h. (E) Western blot analysis of phospho-Zap 70 and Zap 70 in lysates of these cells. (F) FACS analysis of calcium flux in CD4+ T cells in response to anti-CD3 cross-linking. The arrow denotes the time when the stimulus was added to cells.

tested whether AT treatment compromised the TCR–induced activation of ERK and p38 kinases in lymph nodes during EAE. Consistent with effects on Ras and RhoA, in vivo AT treatment blunted the TCR–induced activation of ERK and p38 as well as decreased the DNA-binding of c-fos (a target of ERK and p38) and ATF-2 (a target of p38 and JNK) (Fig. 6, C and D). This effect of AT treatment on T cell ERK and p38 phosphorylation was reversed by cotreatment of mice with farnesol (Fig. S2 B). Consistent with the lack of a major effect of AT on the subcellular localization of Rac1, this drug did not modulate JNK phosphorylation nor the activity of its primary target, c-jun (Fig. 6, C and D). Oral AT treatment also did not inhibit other signaling events triggered by anti-CD3 or anti-CD28 cross-linking including IκB degradation (Fig. 6 C), Zap-70 phosphorylation (Fig. 6 E), and calcium flux (Fig. 6 F).

To test the hypothesis that this inhibition of Ras-ERK and RhoA-p38 signaling by AT was responsible for the Th2 bias induced by this drug, we explored the effects of specific inhibitors of MEK (PD98059), an upstream effector of ERK, and p38 (SB203580) on the antigen–driven differentiation of naive CD4+ cells. Exposure of CD4+ cells to 10 μM of the MEK inhibitor (a dose that does not affect the proliferation or viability of T cells; unpublished data) decreased the production of IFN-γ and increased the secretion of IL-4 by these cells in response to specific peptide (Fig. 7 A). This concentration of PD98059 also reduced the phosphorylation of ERK (Fig. 7 A, bottom). Similarly, exposure of T cells to the p38 kinase inhibitor at doses that inhibit p38 phosphorylation (Fig. 7 B, bottom) and activity (26) induced IL-4 production (only at 0.1 μM) and inhibited IFN-γ production by these cells (Fig. 7 B). The p38 kinase inhibitor also had a more profound effect than the MEK inhibitor in inhibiting T cell proliferation through higher doses tested (10–100 μM) (unpublished data). Collectively, these data support the hypothesis that Ras-ERK and RhoA-p38 signaling pathways are the targets of AT in Th2 differentiation and inhibition of T cell growth.

In vivo treatment with an FTI prevents Th1 differentiation during EAE

In light of the more prominent involvement of protein farnesylation and ERK signaling in regulating the Th1 differentiation of
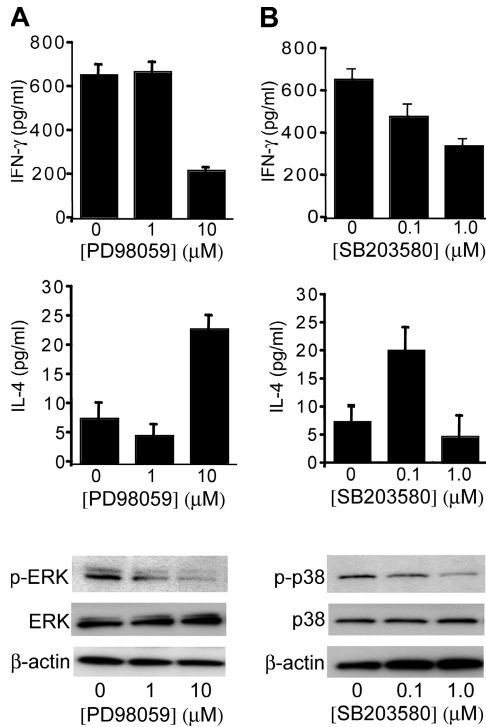
Figure 7. MEK and p38 inhibitors induce Th2 bias of naive CD4+ cells. Naive CD4+ T cells were isolated from spleens of MBP Ac1-11 TCR Tg mice and were cultured with specific peptide in the presence or absence of 5 μg/ml MBP Ac1-11, 1, or 10 μM of the MEK inhibitor PD98059 (A) or 0.1–1 μM of the p38 inhibitor SB203580 (B). Note that these particular doses of MEK or p38 inhibitors did not affect the proliferation or viability of T cells (data not depicted), but did inhibit the phosphorylation of ERK and p38 (bottom). *, denotes a significant (P < 0.05) difference from MBP Ac1-11 stimulated group. β-actin served as a loading control. Values are mean ± SE of triplicate cultures.

Figure 8. In vivo administration of the FTI L–744,832 inhibits Th1 differentiation. Female SJL mice were immunized with PLP p139-151 in CFA and daily were injected s.c. with either vehicle or L-744,832 (30 mg/kg). At day 10 after immunization, spleens were taken from representative mice in each group and isolated splenocytes were cultured ex vivo with PLP p139-151 peptide. (A) The mean ± SE clinical scores of these mice. (B–D) PLP p139-151-stimulated production of IL-2 (B), IFN-γ (C), and TNF-α (D) by isolated splenocytes. Values are mean ± SE of triplicate cultures. *, denotes a significant difference from vehicle control.

MBP-reactive cells in vitro and reports that FTIs (but not GGTIs) are well tolerated in mice (27), we investigated the clinical benefits of the FTI, L-744,832 (30 mg/kg) on the development of EAE (Fig. 8, A–D). We administered the maximum tolerated dose of this drug, which is reported to cause regression of Ras-related tumors in mice (28). Similar to in vitro findings using FTI-277 (Fig. 4 B), IFN-γ production by PLP p139-151–reactive cells from L-744,832–treated mice was markedly reduced compared with control counterparts (Fig. 8 C). Despite this, FTI-treated mice still developed EAE, albeit the day of onset of clinical symptoms for grade one or higher (12.7 ± 0.6 in FTI vs. 11.3 ± 0.6 in vehicle, P < 0.01) and or grade two or higher (19.4 ± 2.0 in FTI vs. 16.0 ± 1.8 in vehicle, P < 0.01) was significantly delayed compared with vehicle controls (Fig. 8 A). The development of inflammation in FTI-treated mice may relate to the fact that this drug caused PLP p139-151–reactive cells to secrete higher amounts of IL-2 (Fig. 8 B), yet did not promote IL-4 secretion (not depicted) nor dampen the production of the proinflammatory cytokine TNF-α by these cells (Fig. 8 D). Collectively, these results
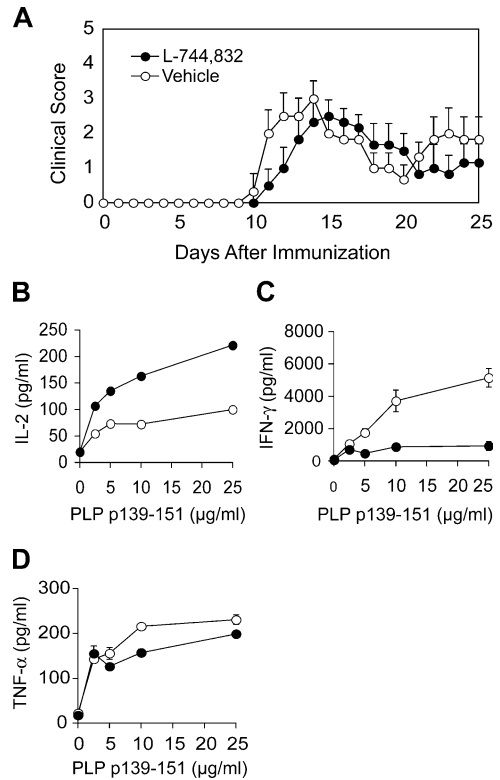
suggest that dual inhibition of protein farnesylation and geranylgeranylation is required to fully promote a Th2 bias of CD4+ cells and prevent the development of CNS inflammation during EAE.

DISCUSSION

Several studies have demonstrated that in vivo statin treatment can cause a protective Th2 bias in animal models of Th1-mediated autoimmune disease (for review see reference 3). These findings have created considerable enthusiasm for testing these agents in patients with MS and rheumatoid arthritis (1, 2). The purpose of the present study was to define the mechanism of immune modulation by this drug. Here, we show that the effect of AT in causing a Th2 bias is the result of a reduction in the biosynthesis of isoprenoids that serve as membrane attachments for Ras and RhoA. Farnesyl-PP, which mediates Ras farnesylation, restored IFN-γ production by AT-treated myelin-reactive T cells, whereas all-trans-geranylgeranyl-PP, the precursor to RhoA geranylgeranylation, reversed the AT block in T cell proliferation and

coordinated with farnesyl–PP to fully reverse the increase in IL-4 promoted by this drug. We also show for the first-time that oral dosing with AT compromised the membrane association of Ras and RhoA GTPases and the TCR-induced activation of targets ERK and p38 in T cells. Inactivation of ERK and p38 signaling mimicked the effects of AT, strongly implicating Ras-ERK and RhoA-p38 pathways as the targets of this drug. Thus, by linking isoprenoid intermediates to two arms of the TCR signaling cascade that modulate T cell cytokine production, we have elucidated a mechanism of how statins may cause a Th2 bias in vivo during EAE.

Our finding that oral dosing with AT caused Ras, RhoA, and Rap GTPases to be preferentially diverted to the cytosol instead of the membrane of lymph node cells in vivo is the first demonstration of its kind. These results thus expand upon previous in vitro reports of lovastatin in tumor cell lines (19, 23, 24) as well as lend concrete support to the prevailing notion that the pleiotrophic effects of statins in treating atherosclerosis and cancer in animal models are the result of reductions in isoprenoid biosynthesis (29–32). Though oral AT administration significantly depleted Ras and RhoA at the membrane of lymph node cells, in comparison, Rap or Rac1 were only marginally affected. The reason for this difference is unclear, but may relate to variations in the half-lives of these proteins (24). Nonetheless, because membrane-association is necessary for the functioning of GTPases, we conclude that Ras and RhoA are the major targets of statin in immune modulation in vivo.

Previous reports have demonstrated that the strength of ERK activation in response to TCR stimulation may influence cytokine production and alter the course of T helper differentiation by altering the binding of c-fos to AP-1 consensus elements (16). Peptides that bind the TCR with strong avidity induce Th1 differentiation of CD4^{+} cells and cause a sustained activation of Ras and ERK that triggers c-fos activity (16, 25). c-fos (with jun as AP-1) appears to repress the IL-4 promoter (16) and coordinates with other transcription factors such as ATF-2 and NFAT to mediate the transactivation of the IFN-γ promoter (26) (Fig. 6 A). However, under conditions when ERK activity is low, such as in the presence of a weak-binding altered peptide ligand (16), or weakened Ras (33), or MEK signaling (16, 34), IFN-γ production is minimal and IL-4 is induced. In this regard, our findings that AT decreased the DNA binding of c-fos and inhibited the activation or Ras-ERK and RhoA-p38 signaling pathways that target this transcription factor provide a mechanistic explanation for the Th2 bias promoted by statins. Interference of p38 activity by AT may have also contributed to this Th2 deviation by reducing the activity of ATF-2 at the IFN-γ promoter (26). In light of this evidence, we propose a model for AT action on T cells in vivo (Fig. 6, compare A and B), whereby this drug selectively inhibits the membrane association of Ras and RhoA leading to decreased activation of ERK and p38 signaling pathways that target AP-1 and ATF-2.

Despite the established role for Ras and ERK in the regulation of IFN-γ production (in this paper and references

16, 33, 34), in vivo FTI treatment only delayed the onset of EAE. These findings emphasize the involvement of geranyl-geranylated proteins in mediating the development of CNS inflammation. Indeed, our data indicate a role for geranyl-geranylated Rho proteins in mediating the proliferation of encephalitogenic T cells. These results thus correspond with previous reports that statins cause G1 arrest (35) and that geranylgeranylated proteins regulate the G1 to S transition (36). We also found that inhibition of protein geranylgera-nylation in myelin-reactive cells was requisite for full induction of IL-4 and was likely required for the attenuation of TNF-α production by AT (i.e., AT [reference 5], but not FTI treatment diminishes T cell production of this cytokine). These findings, coupled with the established involvement of geranylgeranylated Rho proteins in regulating the transmigration of T cells across brain endothelium (7), emphasize that dual inhibition of farnesylation and geranyl-geranylation by statins is necessary to prevent the development of CNS autoimmunity.

Although reducing the production of farnesyl–PP by AT hindered T cell growth and Th1 differentiation, in vivo treatments that cause increased incorporation of this metabolite into prenylated proteins, such as farnesol (17) or Zaragozic Acid A (18, 37), induced pathogenic myelin-reactive T cells to proliferate more vigorously, secrete higher amounts of IFN-γ, and precipitate worse EAE. Thus, accumulation of farnesyl–PP may enhance Th1-mediated inflammation in vivo. Though we observed in vitro Zaragozic Acid A treatment to trigger an increased accumulation of farnesyl–PP in T cells, it remains unclear whether this also occurred in mice in response to in vivo treatment or whether it was the increased liver production of farnesyl–PP–derived lipids (18, 37) that was responsible for the immune modulatory effects of this drug. The latter possibility (i.e., that the liver production of isoprenoids can boost adaptive immune responses) is provocative and provides an interesting correlate to reports that metabolic precursors in the mevalonate pathway are preferentially diverted toward isoprenoid as opposed to sterol biosynthesis in the liver during the acute phase response to inflammatory stimuli (38, 39).

In conclusion, we show that farnesylated Ras and gera-nylgeranylated RhoA proteins are the targets of AT in immune modulation in vivo. Our results also underscore that inhibition of both protein farnesylation and geranylgeranylation in T cells is key to promoting a Th2 bias and preventing the development of EAE. Because oral AT administration is well tolerated, whereas continuous and combined FTI and GGTI therapy is toxic in vivo (27), we maintain that of these, statin treatment is a more promising approach than selective inhibition of individual prenyltransferases for treatment of MS and other Th1-mediated autoimmune diseases.

MATERIALS AND METHODS
Reagents. Mevalonate, farnesol, farnesyl–PP, all-trans geranylgeranyl–PP, ubiquinone, Zaragozic Acid A, β-methyl cyclodextrin, and filipin were obtained from Sigma-Aldrich. Cold 2-cis geranylgeraniol, [acetyl-³H] acetyl CoA (20 Ci/mmol), and [1-³H] farnesyl–PP (60 Ci/mmol) were obtained

from American Radiochemicals. Purified AT was a gift from R. Laskey (Pfizer, New York, NY). FTI-277, GGTI-298, L-744,832, SB203580, and PD98059 were obtained from Calbiochem. Fluo-4 was obtained from Invitrogen. Peptides encoding myelin basic protein (MBP), Ac1–11 (Ac-ASQKRPSQRHG), or proteolipid protein (PLP) p139–151 (HCLGK-WLGHPDKF) were synthesized by the Stanford Pan Facility and purified by HPLC. Pan Ras (clone 18) and Rac1 (clone 102) antibodies were obtained from BD Transduction Labs. RhoA (clone 26C4), Rap1 (clone sc-65), T-bet (clone sc-21749), and GATA-3 (clone sc-268) antibodies were obtained from Santa Cruz Biotechnology, Inc. Phospho(p42/44)-ERK (no. 9101S), p42/p44 MAPK (no. 9102), phospho-JNK (no. 9251S), JNK (no. 9252), phospho-p38 (no. 9216S), p38 (no. 9212), phospho-Zap-70 (no. 2701), and IκBα (no. 9242) antibodies were all obtained from Cell Signaling. The pan-Zap-70 antibody (clone 1E7.2) was obtained from Upstate Biotechnology. Goat anti–mouse IgG antibody was obtained from Jackson Immuno-Research Laboratories.

Mice. Female SJL/J and (PL/J × SJ/L)$_{F1}$ mice (6–10 wk old) were purchased from The Jackson Laboratory. MBP Ac1-11 TCR Tg mice backcrossed onto the B10.PL background (40) were maintained in our animal facility. All animal protocols were approved by the Division of Comparative Medicine at Stanford University and the Committee of Animal Research at the University of California San Francisco and animals were maintained in accordance with the guidelines of the National Institutes of Health.

EAE induction. EAE was induced in SJL/J mice via subcutaneous immunization with 100 μg PLP p139-151 in an emulsion (volume ratio 1:1) with CFA containing 4 mg/ml of heat-killed *Mycobacterium tuberculosis* H37Ra (Difco Laboratories). (PL/J × SJ/L)$_{F1}$ mice were immunized with MBP Ac1-11 in CFA. Mice ($n = 10$ per treatment group) were examined daily for clinical signs of EAE and were scored as followed: 0 = no clinical disease, 1 = limp tail, 2 = hindlimb weakness, 3 = complete hindlimb paralysis, 4 = hindlimb paralysis plus some forelimb paralysis, and 5 = moribund or dead.

In vivo drug treatments. AT (prescription formulation; Pfizer) was brought into suspension in PBS (0.4 mg/ml) and a 0.5-ml volume of this suspension (equivalent to 10 mg/kg) was administered to mice orally, once daily, using 20-mm feeding needles (Popper and Sons, Inc). Farnesol (undiluted lipid, 5 mg/kg) and Zaragozic Acid A (dissolved in saline, 10 mg/kg) were injected i.p. once daily. The specific inhibitor of farnesyltransferase, L-744,832, was dissolved in 0.9% saline (pH 5.4, 30 mg/kg) and injected subcutaneously, once daily. Mice treated with appropriate vehicles served as controls. All treatments were initiated at 2 d before immunization, and splenocyte and lymph node cells were harvested from representative mice in each group at 10 d after disease induction.

Proliferation assays and cytokine analysis. Splenocytes (0.5×10^6 cells/well), lymph node cells (0.5×10^6 cells/well), or CD4$^+$ T cells (5×10^4 cells/well) purified by negative selection (columns from R&D Systems) were cultured in flat-bottomed, 96-well plates with appropriate peptide (1–25 μg/ml) and irradiated splenocytes (in the case of purified CD4$^+$ cells) or were stimulated with 2 or 5 μg/ml each of αCD3 (clone 145-2C11; BD Biosciences) and αCD28 (clone 37.51; BD Biosciences). Culture medium consisted of RPMI 1640 supplemented with L-glutamine (2 mM), sodium pyruvate (1 mM), nonessential amino acids (0.1 mM), penicillin (100 U/ml), streptomycin (0.1 mg/ml), 2-mercaptoethanol (5×10^{-5} M), and 10% fetal calf serum. After 48–72 h, cultures were pulsed with [^{3}H]thymidine (1 μCi/well) and 18 h later were harvested onto filter paper. The cpm of incorporated [^{3}H]thymidine were read using a β-counter. Cytokines were measured in the supernatants of cultured cells using anti–mouse OPTEIA ELISA kits (BD Biosciences). Supernatants were taken at the time of peak production for each cytokine: IL-2 (48 h), IFN-γ (72 h), TNF-α (72 h), and IL-4 (120 h).

Analysis of HMG-CoA reductase mRNA expression via real-time RT-PCR. Total RNA was isolated from liver using the Absolutely RNA RT-PCR Miniprep kit (Statagene). 1 μg of RNA was reverse-transcribed and HMG-CoA reductase and β actin cDNAs amplified according to previous methods (41) using a Lightcycler (Roche). Primer sequences were as follows: HMG-CoA reductase (sense): 5′-TTCTGGCAGTCAGTGGG-3′; HMG-CoA reductase (antisense): 5-CAATGTTTGCTGCGTGG-3′; β-actin (sense): 5′-GAACCCTAAGGCCAACGCT-3′; and β-actin (antisense): 5′-CACGCACGATTTCCCTCTC-3′.

T cell cholesterol extraction and amplex red assay. Total cholesterol was extracted from cells using the Heider and Boyett method (42). In brief, purified cells (10×10^6) were suspended in 500 μl of isopropanol and sonicated for 15 s using a microprobe. Samples were centrifuged at 800 g for 15 min to precipitate cellular proteins. The supernatant containing the cholesterol was decanted to a clean tube, evaporated to dryness, and resuspended in 1× reaction buffer. The remaining protein pellet was suspended in 100 μl of 0.1 M sodium hydroxide and used for protein determination. Total cholesterol was measured in the lipid extract and in serum of mice using Amplex Red Cholesterol Assay kit (Invitrogen).

FACS analysis of filipin staining. Membrane-associated cholesterol was determined in T cells by measuring filipin fluorescence (43). T cells (10^6) were first fixed in 120 μl of 4% paraformaldehyde at room temperature for 12 min, washed three times in 1× PBS, and incubated with the dye (1:100 of 25 mg/ml filipin stock) for 1 h at 4°C. Samples were washed three times with 1× PBS and filipin fluorescence was measured using a FACS Vantage SE/Diva (BD Biosciences) with the krypton ion laser tuned to UV (350.7–356.4 nm) and emission detection at 420–460 nm. Data were analyzed using FloJo software (Ver. 6.3.3) (Treestar).

Metabolic labeling. De novo incorporation of farnesyl-PP into T cell proteins was assessed using a modified procedure of Corsini et al. (44). In brief, purified T cells (3×10^6/ml in stimulation media) were cultured in six-well plates coated with anti-CD3 (5 μg/ml) and anti-CD28 (5 μg/ml) in the absence or presence of 200 μM Zaragozic Acid A. After 12 h, T cells were pulsed with [1-^{3}H] farnesyl-PP (60 Ci/mmol) and cultured for additional 20 h. For each condition, cells were pooled and washed three times in 1× PBS (containing 1 mM PMSF). After the final centrifuge (1,200 revolutions/min for 5 min), cells were resuspended in 1× PBS and sonicated for 15 s using a microprobe. Cellular proteins were delipidated (44), 60 μg of protein was subjected to SDS-PAGE, and gels were stained with Coomassie blue to visualize proteins. Gels were then treated with Amplify for 30 min, washed, dried, and exposed to a Tritium K-Screen (Kodak) for 3 wk. Exposure of the screen was detected using a Fx Pro-Plus Molecular Imager and Quantity One software (both obtained from Bio-Rad Laboratories).

Cell fractionation and protein isolation. For extraction of total cell protein, splenocytes or lymph node cells were dissociated from surrounding connective tissue, red blood cells were lysed, and cells were counted and resuspended in an appropriate volume (10 μl/million cells) of NP-40 buffer (150 mM NaCl, 1 mM EDTA, 1 mM EGTA, 1% Triton X-100, 2.5 mM Na$_2$PO$_4$, 1 mM glycerol phosphate, 1 mM Na$_3$V0$_4$, 1 g/ml leupeptin, 1 mM PMSF, Roche protease inhibitor tablet, 20 mM Tris, pH 7.5). After a 30-min extraction on ice, samples were centrifuged at 15,000 g for 15 min at 4°C to obtain a clarified supernatant. For cell fractionation studies, splenocyte or lymph node cells were homogenized in lysis buffer (1 mM EDTA, 20 mM Tris-HCl, pH 7.4) using a glass homogenizer and were centrifuged at 100,000 g using a Beckman ultracentrifuge. The supernatant (soluble fraction) was concentrated using a 10 K molecular limit Nanosep centrifugal device (Pall Life Sciences). The membrane pellet was solubilized in 1× immunoprecipitation buffer (0.15 M NaCl, 1% Triton X-100, 0.5% sodium deoxycholate, and 0.1% SDS, 10 mM Tris-HCl, pH 7.5) and centrifuged at 15,000 g to obtain a clarified supernatant. Proteinase inhibitors were included in all buffers. Nuclear extracts from lymph nodes cells were isolated using the BD Transfactor Extraction Kit (CLONTECH Laboratories, Inc.) according to kit directions. The concentration of proteins in each sample

was determined using a BCA assay kit (Pierce Chemical Co.). DNA binding assays were conducted using a commercial ELISA kit (CLONTECH Laboratories, Inc.).

SDS–PAGE and Western analysis. Each protein sample was suspended in 2 vol. of 2× SDS Sample Buffer (Bio-Rad Laboratories) and subjected to SDS-PAGE electrophoresis using precast Tris-HCl Ready-Gels (Bio-Rad Laboratories). Proteins were transferred to PVDF membranes (GE Healthcare) and immunoblotting was performed using conventional methods (Santa Cruz Biotechnology, Inc.).

Calcium flux analysis. Calcium flux in CD4$^+$ T cells was measured after CD3 cross-linking using a FACScan (BD Biosciences) (45). In brief, CD4$^+$ cells purified from spleens of mice (10^6/ml), were washed in 1× PBS and loaded with Fluo-4 (2 μM) in the presence of CaCl$_2$ (2 mM) for 20 min at room temperature. Cells were washed twice with 1× PBS, resuspended at a concentration of 2 × 10^6/ml in FACS buffer, and placed in a 37°C water bath. Samples (37°C) were first acquired for 30 s to establish baseline fluorescence in FL1 channel before the addition of anti-CD3 (5 μg/ml) and the goat anti–mouse IgG (10 μg/ml). After stimulation, events were collected for an additional 10 min. Data were analyzed using the kinetics platform in FloJo software (Ver. 6.3.3).

Statistical analysis. Data are presented as means ± SE. When data were parametric, a one-way analysis of variance and a Scheffé post-hoc test (for >2 groups) or a Student's t test ($n = 2$ groups) were used to detect between-group differences. When data were nonparametric, ranks were compared amongst groups using a Kruskal-Wallis test and nonparametric test for multiple comparisons (for >2 groups) or a Mann-Whitney U test ($n = 2$ groups). A value of $P < 0.05$ was considered significant.

Online supplemental material. Fig. S1 shows the influence of AT and isoprenoid metabolites on the proliferation of and cytokine production by purified T cells in culture. Fig. S2 shows how in vivo treatment with farnesol can reverse the effects of AT on the membrane localization of Ras and RhoA and the TCR-induced phosphorylation of ERK and p38 in lymph node cells. Tables S1 and S2 summarize the clinical features of EAE in experiments depicted in Figs. 1 and 3. Online supplemental material is available at http://www.jem.org/cgi/content/full/jem.20051129/DC1.

REFERENCES

1. Vollmer, T., L. Key, V. Durkalski, W. Tyor, and J. Corboy. 2004. Oral simvastatin treatment in relapsing-remitting multiple sclerosis. *Lancet.* 363:1607–1608.
2. McCarey, D.W., I.B. McInnes, R. Madhok, R. Hampson, O. Scherbakov, I. Ford, H.A. Capell, and N. Sattar. 2004. Trial of atorvastatin in Rheumatoid Arthritis (TARA): double-blind, randomised placebo-controlled trial. *Lancet.* 363:2015–2021.
3. Neuhaus, O., O. Stuve, S.S. Zamvil, and H.-P. Hartung. 2004. Are statins a treatment option for multiple sclerosis? *Lancet Neurol.* 3:369–371.
4. Stanislaus, R., K. Pahan, A.K. Singh, and I. Singh. 1999. Amelioration of experimental allergic encephalomyelitis in Lewis rats by lovastatin. *Neurosci. Lett.* 269:71–74.
5. Youssef, S., O. Stuve, J.C. Patarroyo, P.J. Ruiz, J.L. Radosevich, E.M. Hur, M. Bravo, D. Mitchell, R.A. Sobel, L. Steinman, and S.S. Zamvil. 2002. The HMG-CoA reductase inhibitor atorvastatin, promotes Th2 bias and reverses paralysis in central nervous system autoimmune disease. *Nature.* 420:78–84.
6. Aktas, O., S. Waiczies, A. Smorodchenko, J. Dorr, B. Seeger, T. Prozorovski, S. Sallach, M. Endres, S. Brocke, R. Nitsch, and F. Zipp. 2003. Treatment of relapsing paralysis in experimental encephalomyelitis by targeting Th1 cells through atorvastatin. *J. Exp. Med.* 197:725–733.
7. Greenwood, J., C.E. Walters, G. Pryce, N. Kanuga, E. Beraud, D. Baker, and P. Adamson. 2003. Lovastatin inhibits brain endothelial Rho-mediated lymphocyte migation and attenuates experimental autoimmune encephalomyelitis. *FASEB J.* 17:905–907.
8. Nath, N., S. Giri, R. Prasad, A.K. Singh, and I. Singh. 2004. Potential targets of 3-hydroxy-3-methylglutaryl Coenzyme A reductase inhibitor for multiple sclerosis therapy. *J. Immunol.* 172:1273–1286.
9. Leung, B.P., N. Sattar, A. Crilly, M. Prach, D.W. McCarey, H. Payne, R. Madhok, C. Campbell, J.A. Gracie, F.Y. Liew, and I.B. McInnes. 2003. A novel anti-inflammatory role for simvastatin in inflammatory arthritis. *J. Immunol.* 170:1524–1530.
10. Gegg, M.E., R. Harry, D. Hankey, H. Zambarakji, G. Pryce, D. Baker, P. Adamson, V. Calder, and J. Greenwood. 2005. Suppression of autoimmune retinal disease by lovastatin does not require Th2 cytokine induction. *J. Immunol.* 174:2327–2335.
11. Shimada, K., K. Miyauchi, and H. Daida. 2004. Early intervention with atorvastatin modulates TH1/TH2 imbalance in patients with acute coronary syndrome: from bedside to bench. *Circulation.* 109:e213–e214.
12. Topol, E.J. 2004. Intensive statin therapy-a sea change in cardiovascular prevention. *N. Engl. J. Med.* 350:1562–1564.
13. Goldstein, J.L., and M.S. Brown. 1990. Regulation of the mevalonate pathway. *Nature.* 343:425–430.
14. Grunler, J., J. Ericsson, and G. Dallner. 1994. Branch-point reactions in the biosynthesis of cholesterol, dolichol, ubiquinone, and prenylated proteins. *Biochim. Biophys. Acta.* 1212:259–277.
15. Weitz-Schmidt, G., K. Welzenbach, V. Brinkmann, T. Kamata, J. Kallen, C. Bruns, S. Cottens, Y. Takada, and U. Hommel. 2001. Statins selectively inhibit leukocyte function antigen-1 by binding to a novel regulatory integrin site. *Nat. Med.* 7:687–692.
16. Jorritsma, P.J., J.L. Brogdon, and K. Bottomly. 2003. Role of TCR-induced extracellular signal-related kinase activation in the regulation of early IL-4 expression in naïve CD4$^+$ T cells. *J. Immunol.* 170:2427–2434.
17. Ownby, S.E., and R. Hohl. 2002. Farnesol and geranylgeraniol: prevention and reversion of lovastatin-induced effects in NIH3T3 cells. *Lipids.* 37:185–192.
18. Balamuth, F., D. Leitenberg, J. Unternaechrer, I. Mellman, and K. Bottomly. 2001. Distinct patterns of membrane microdomain partitioning in Th1 and Th2 cells. *Immunity.* 15:729–738.
19. Ghittoni, R., L. Patrussi, K. Pirozzi, M. Pellegrini, P.E. Lazzerini, P.L. Capecchi, F.L. Pasini, and C.T. Baldari. 2005. Simvastatin inhibits T-cell activation by selectively impairing the function of Ras superfamily GTPases. *FASEB J.* 19:605–607.
20. Vaidya, S., R. Bostedor, M.M. Kurtz, J.D. Bergstrom, and V.S. Bansal. 1998. Massive production of farnesol-derived dicarboxylic acids in mice treated with the squalene synthetase inhibitor Zaragozic Acid A. *Arch. Biochem. Biophys.* 355:84–92.
21. Zhang, F.L., and P.J. Casey. 1996. Protein prenylation: molecular mechanisms and functional consequences. *Annu. Rev. Biochem.* 65:241–269.
22. Cantrell, D.A. 2003. GTPases and T cell activation. *Immunol. Rev.* 192:122–130.
23. Goldman, F., R.J. Hohl, J. Crabtree, K. Lewis-Tibesar, and G. Koretzky. 1996. Lovastatin inhibits T-cell antigen receptor signaling independent of its effects on ras. *Blood.* 88:4611–4619.
24. Holstein, S.A., C.L. Wohlford-Lenane, and R.J. Hohl. 2002. Consequences of mevalonate depletions: differential transcriptional, translational, and posttranslational upregulation of Ras, Rap1a, RhoA, and RhoB. *J. Biol. Chem.* 277:10678–10682.
25. Badou, A., M. Savignac, M. Moreau, C. Leclerc, G. Foucras, G. Cassar, P. Paulet, D. Lagrange, P. Druet, J.C. Guery, and L. Pelletier. 2001. Weak TCR stimulation induces a calcium signal that triggers IL-4

synthesis, stronger TCR stimulation induces MAP kinases that control IFN-γ production. *Eur. J. Immunol.* 31:2487–2496.

26. Rincon, M., and R.A. Flavell. 1999. Reprogramming transcription during the differentiation of precursor CD4+ cells into effector Th1 and Th2 cells. *Microbes Infect.* 1:43–50.

27. Lobell, R.B., C.A. Omer, M.T. Abrams, H.G. Bhimnathwala, M.J. Brucker, C.A. Buser, J.P. Davide, S.J. deSolms, C.J. Dinsmore, M.S. Ellis-Hutchings, et al. 2001. Evaluation of farnesyl:protein transferase and geranylgeranyl:protein transferase inhibitor combinations in pre-clinical models. *Cancer Res.* 61:8758–8768.

28. Kohl, N.E., C.A. Omer, M.W. Conner, N.J. Anthony, J.P. Davide, S.J. deSolms, E.A. Giuliani, R.P. Gomez, S.L Graham, and K. Hamilton. 1995. Inhibition of farnesyltransferase induces regression of mammary and salivary carcinomas in ras transgenic mice. *Nat. Med.* 1:792–797.

29. Mach, F. 2004. Statins as immunomodulatory agents. *Circulation.* 109:II15–II17.

30. Bellosta, S., N. Ferri, F. Bernini, R. Paoletti, and A. Corsini. 2000. Non-lipid related effects of statins. *Ann. Med.* 32:164–176.

31. Mo, H., and C.E. Elson. 2004. Studies of the isoprenoid-mediated inhibition of mevalonate synthesis applied to cancer chemotherapy and chemoprevention. *Exp. Biol. Med (Maywood).* 229:567–585.

32. Liao, J.K. 2002. Isoprenoids as mediators of the biological effects of statins. *J. Clin. Invest.* 110:285–288.

33. Layer, K., G. Lin, A. Nencioni, W. Hu, A. Schmucker, A.N. Antov, X. Li, S. Takamatsu, T. Chevassut, N.A. Dower, et al. 2003. Autoimmunity as a consequence of a spontaneous mutation in Rasgrp 1. *Immunity.* 19:243–255.

34. Dumont, F.J., M.J. Staruch, P. Fischer, C. DaSilva, and R. Camacho. 1998. Inhibition of T cell activation by pharmacological disruption of the MEK1/ERK kinase or calcineurin signaling pathways results in differential modulation of cytokine production. *J. Immunol.* 160:2579–2589.

35. Naderi, S., R. Blomhoff, J. Myklebust, E.B. Smeland, B. Erikstein, K.R. Norum, and H.K. Blomhoff. 1999. Lovastatin inhibits G1/S transition of normal human B-lymphocytes independent of apoptosis. *Exp. Cell Res.* 252:144–153.

36. Vogt, A., Y. Qian, T.F. McGuire, A.D. Hamilton, and S.M. Sebti. 1996. Protein geranylgeranylation, but not farnesylation is required for the G1 to S transition in mouse fibroblasts. *Oncogene.* 13:1991–1999.

37. Bergstrom, J.D., M.M. Kurtz, D.J. Rew, A.M. Amend, J.D. Karkas, R.G. Bostedor, V.S. Bansal, C. Dufresne, F.L. VanMiddlesworth, and O.D. Hensens. 1993. Zaragozic acids: a family of metabolites that are picomolar competitive inhibitors of squalene synthetase. *Proc. Natl. Acad. Sci. USA.* 90:80–84.

38. Hardardottir, I., A.H. Moser, R. Memon, C. Grunfeld, and K.R. Feingold. 1994. Effects of TNF, IL-1, and the combination of both cytokines on cholesterol metabolism in Syrian hamsters. *Lymphokine Cytokine Res.* 13:161–166.

39. Memon, R.A., I. Shechter, A.H. Moser, J.K. Shigenaga, C. Grunfeld, and K.R. Feingold. 1997. Endotoxin, tumor necrosis factor, and interleukin-1 decrease hepatic squalene synthase activity, protein, and mRNA levels in Syrian hamsters. *J. Lipid Res.* 38:1620–1629.

40. Hardardottir, F., J.L. Baron, and C.A. Janeway Jr. 1995. T cells with two functional antigen-specific receptors. *Proc. Natl. Acad. Sci. USA.* 92:354–358.

41. Pedotti, R., J.J. DeVoss, S. Youssef, D. Mitchell, J. Wedemeyer, R. Madanat, H. Garren, P. Fontoura, M. Tsai, S.J. Galli, et al. 2003. Multiple elements of the allergic arm of the immune response modulate autoimmune demyelination. *Proc. Natl. Acad. Sci. USA.* 100:1867–1872.

42. Heider, J.G., and R.L. Boyett. 1978. The picomole determination of free and total cholesterol in cells in culture. *J. Lipid Res.* 19:514–518.

43. Karnell, F.G., R.J. Brezski, L.B. King, M.A. Silverman, and J.G. Monroe. 2005. Membrane cholesterol content accounts for developmental differences in surface B cell receptor compartmentalization and signaling. *J. Biol. Chem.* 280:25621–25628.

44. Corsini, A., C.C. Farnsworth, P. McGeady, M.H. Gelb, and J.A. Glomset. 1999. Incorporation of radiolabeled prenyl alcohols and their analogs into mammalian cell proteins. *Methods Mol. Biol.* 116:125–144.

45. Smith, K., B. Seddon, M.A. Purhboo, R. Zamoyska, A.G. Fisher, and M. Merkenschlager. 2001. Sensory adaptations in naive peripheral CD4 T cells. *J. Exp. Med.* 194:1253–1262.

412

ATORVASTATIN INDUCES TH2 BIAS BY INHIBITING RAS AND RHOA | Dunn et al.